IEEE Access
Multidisciplinary | Rapid Review | Open Access Journal

Received April 19, 2021, accepted May 8, 2021, date of publication May 19, 2021, date of current version June 2, 2021.

Digital Object Identifier 10.1109/ACCESS.2021.3081924

Control Strategy for Electric Startup of P2.5-PHEV Based on Slope Memory and Driver's Startup Intention

YONG LUO[1], YONGHENG WEI[1], YINGZHE KAN[2], LIN REN[1], LIJI XU[1], FUTAO SHEN[1], AND GUOFANG CHEN[1]

[1]Key Laboratory of Advanced Manufacturing Technology for Automobile Parts, Ministry of Education, Chongqing University of Technology, Chongqing 400054, China
[2]State Key Laboratory of Mechanical Transmission, Chongqing University, Chongqing 400044, China

Corresponding author: Yongheng Wei (weiyongheng1995@163.com)

This work was supported in part by the China National Natural Science Foundation under Grant 51305475, in part by the Chongqing Program of Basic Research and Frontier Technology under Grant cstc2019jcyj-msxmX0308, in part by the Scientific Program of Chongqing Municipal Education Commission under Grant KJQN201801143, and in part by the Scientific Research Support Project of the Vehicle Engineering College of CQUT under Grant CL2019-16.

ABSTRACT P2.5 plug-in hybrid electric vehicles (P2.5-PHEVs) exhibit high transmission efficiencies and no power interruption in the shifting and mode switching process; thus, they have broad application prospects. The power transmission in a PHEV under pure electric startup does not entail the clutch, and the initial torque of the motor is often set under the condition that the maximum allowable slope should not lead to backward sliding, which leads to the problems of excessive jerk in small-slope startup and catapulting when startup occurs downhill. The optimal method is to set different initial torques according to different gradients; however, the vehicle would still be in the pre-startup stage, making it impossible to estimate the slope using a dynamic method. In view of the foregoing problems, according to an analysis of pure electric startup dynamics, a slope-memory-based strategy for estimating and storing the slope during the vehicle movement before parking is proposed. During startup, the initial torque is set according to the memorized slope. In the processes of startup and acceleration, the driver's startup intention is identified, and different jerk control targets are set. The torque of the acceleration process is controlled according to the set initial torque and jerk target. Simulation results indicate that the maximum jerk of the proposed strategy is reduced by 23.6% for startup on a 5% ramp and by 57.5% for startup at 15% downhill; thus, the strategy mitigates the problems of the excessive jerk and catapult for startup on a small slope.

INDEX TERMS P2.5 hybrid powertrain configuration, road slope estimation, startup intention identification, vehicle startup process.

I. INTRODUCTION

With increasingly severe energy crises and environmental pollution, fuel consumption and emission regulations are becoming more stringent, and new vehicles based on different types of energy have ushered in broader development prospects [1]. Owing to the limitations of battery energy densities, the range anxiety problem related to pure electric vehicles (EVs) is difficult to solve in the short term. Plug-in hybrid electric vehicles (PHEVs) have more market-oriented advantages. Major automobile manufacturers have invested in the development of PHEVs, and plug-in hybrid power systems (PHPSs) with different configurations have appeared on the market [2]–[4]. Owing to the structural characteristics of the dual input shaft, the need to avoid power interruption, and the high transmission efficiency, the proportion of dual-clutch transmissions (DCTs) in the current PHPSs has increased annually [5], [6].

Hybrid power systems can be classified in various ways; generally, P (position) is used to represent the structure and motor position of electrified components. Single-motor hybrid systems are classified as P1, P2, P2.5, P3, P4, and other configurations [7]. In the P2.5 configuration equipped with a DCT, the motor is significantly integrated into the

The associate editor coordinating the review of this manuscript and approving it for publication was Shiwei Xia.

input shaft of the DCT. In contrast with the P1 configuration, wherein the motor is placed at the output end of the engine, and the P2 configuration, wherein the motor is placed at the input end of the gearbox, the P2.5 configuration provides parking power generation. The motor efficiency is not affected by the high-temperature thermal radiation from the engine. The P2.5-motor torque can be directly transferred via the transmission to start or drive a P2.5 PHEV, and the clutch controls the engine power transmission. Furthermore, in contrast with the P3 and P4 configurations, wherein the motor is located at the output end of the gearbox, the P2.5 configuration optimizes the working range of the motor by using part of the variable speed ratio of the transmission. Moreover, this configuration improves the power output efficiency, avoids the need for a low-voltage motor to start the engine, generates electricity, leads to a small vehicle jerk arising from the coupled use of oil and electricity, and provides improved driving comfort [8], [9]. Therefore, owing to its various advantages, the P2.5 configuration based on a DCT has broad application prospects and research significance.

The startup process, an important part of a vehicle's dynamic operation, has continually been a research focus and has entailed difficulties in the driving processes of dynamic vehicles [10]. Scholars worldwide have conducted extensive research for improving the control quality of the pure electric startup process. In past research, the pure electric startup process was controlled according to the comfort and subjective feelings of drivers and passengers [11]–[13]. These studies mainly considered the comfort of drivers and passengers, vehicle performance requirements, etc.; however, they did not consider the vehicle jerk in slopes or the driver's startup intentions. In view of the foregoing problems, in [14], [15], and [16], different environments and working conditions were considered for vehicles during startup—specifically, startup slopes of different types and sizes were considered. In addition to the vehicle load and other factors, the value of the slope was approximately determined via slope estimation after movement, and subsequently, the startup torque was modified according to different values of the slope to improve the startup performance. However, problems such as sliding backward and catapulting can easily arise during the period from the vehicle movement to the calculation of the slope. According to this observation, Yang *et al.* [17] analyzed the slope and driver's startup intention and applied initial startup torques with and without pedal opening, respectively. Although this approach can ensure that the vehicle does not slide backward on a small uphill slope, the startup torque cannot adapt to the influence of the slope change. When the startup occurs on a small uphill or downhill slope, it can easily cause evident catapulting or vehicle jerk, affecting the quality of the startup process.

As indicated by the foregoing analysis, the current research mainly focuses on improving the accuracy of slope estimation, startup performance, and comfort of drivers and passengers. In the current pure electric startup approach, the initial torque of the motor is usually set under the condition that the maximum allowable slope does not lead to sliding backwards; this leads to the problems of excessively large vehicle jerk in small-slope startups and catapulting when the startup occurs downhill. The optimal method is to set different initial torques according to different slopes, but the vehicle is stationary before startup; therefore, the slope cannot be estimated using a dynamic method. However, it can be determined approximately; for example, through slope estimation. The initial torque is set according to the maximum allowable slope, and the torque is adjusted according to the driver's startup intention. When the gradient changes, it cannot satisfy the driver's real startup demand.

In this study, a P2.5-PHEV equipped with a DCT is employed to solve the aforementioned problems. The motor is placed behind the clutch as there is no need to engage the clutch during the pure electric startup process; therefore, it is not necessary to consider the sliding friction work and/or transmission efficiency corresponding to the clutch engagement process. Thus, a pure electric startup control strategy based on slope memory and startup intention recognition is proposed. According to the last parking time before startup, the slope value is calculated and stored in the controller. When the vehicle starts, the slope value is read, and the startup anti-slide backward torque is determined for the adaptive slope. Simultaneously, by considering the driver's startup demand according to the accelerator pedal opening and its change rate, the driver's startup intention is identified. It can be divided into three types: slow start, normal start, and fast start. The corresponding pedal types for providing the required torque during the startup process are soft pedal, linear pedal, and hard pedal, respectively. Targeting the degree of vehicle jerk, the startup intention is combined with the slope value to provide an adaptive compensation torque for preventing catapulting and excessive vehicle jerk.

This paper is structured as follows. Section 1 discusses the research background and progress in recent years, along with the research content of the present paper. Section 2 introduces the structure and working principle of the P2.5-PHPS. In Section 3, we analyze the pure electric startup process dynamics of the P2.5-PHPS and the evaluation index. In Section 4, we establish a pure electric startup control strategy for P2.5-PHPS that is based on the slope memory and recognition of the driver's startup intention. We summarize and analyze the results in Section 5.

II. MODELING OF P2.5-PHPS

A. P2.5-PHPS STRUCTURE AND PRINCIPLE

The research object of this study is a P2.5-PHPS equipped with a DCT, and it comprises a P2.5-motor, an engine, a wet DCT, a final drive, and other subsystems. A structural diagram of the powertrain systems is shown in Fig. 1.

As shown in Fig. 1, the DCT has two input shafts in a coaxial line; the first input shaft is nested in the hollow second input shaft. Further, the first input shaft is a solid shaft and is connected to Clutch 1 (C1) through the splines.

TABLE 1. Basic parameters of the vehicle.

Item	Parameters	Valve
Vehicle	Vehicle mass(Kg)	1580
	Tire rolling radius(m)	0.308
	Windward area(m^2)	2.226
	Rolling resistance coefficient	0.015
	Drag coefficient	0.31
P2.5-motor	Maximum torque(N.m)	172
	Peak power(kW)	80
DCT	1^{st} /2^{nd} gear to wheel end ratio(Engine)	13.95/7.466
	1^{st} gear to wheel end speed ratio(P2.5-motor)	8.245

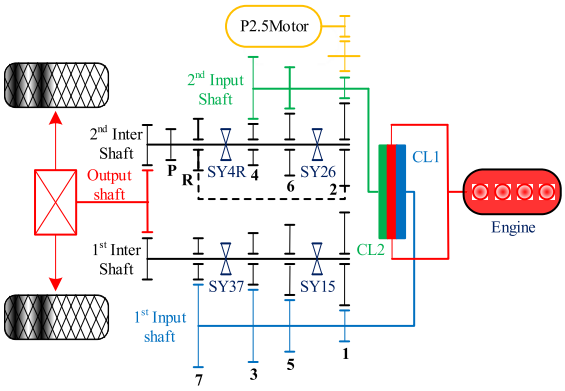

FIGURE 1. Structural diagram of the P2.5-PHPS equipped with a DCT.

The 1^{st}, 3^{rd}, 5^{th}, and 7^{th} driving gears are installed on input shaft 1, and the 2^{nd}, 4^{th}, 6^{th}, and R driving gears are installed on input shaft 2. The power source of the system comprises an engine and a P2.5-motor. The engine is connected to Clutch 1 (C1) and Clutch 2 (C2). The P2.5-motor is placed behind the clutch and is integrated into the DCT. It is connected to the second input shaft (even shaft) of the DCT and can share the 2^{nd}, 4^{th}, and 6^{th} gears. When C2 is used, the engine can drive the vehicle alone, and the P2.5-motor can output the driving torque through the input shaft. When C1 is used, the engine can not only drive the vehicle alone but also output the driving torque through the second input shaft together with the P2.5-motor.

By analyzing the structure of the P2.5-PHPS equipped with a DCT, basic parameters of the vehicle were obtained, as shown in Table 1.

B. P2.5-MOTOR CHARACTERISTIC MODEL

The power source of the P2.5-PHPS includes the engine and the P2.5-motor. The pure electric drive (including the pure electric startup and P2.5-motor) is used as a power source to provide the torque required for the vehicle.

The P2.5-motor characteristic model is shown in Fig. 2. Using the relevant experimental data of the P2.5-motor obtained from a bench test, the relationships among the torque, speed, and efficiency of the P2.5-motor were determined through an interpolation method and are shown in Fig. 2(a). The characteristic curves of the peak torque, sustainable output torque, peak power, and sustainable output power are presented in Fig. 2(b). As shown, for the majority of the working area, the efficiency of the P2.5-motor was maintained in the range of 85%–90%, and the highest efficiency was 96%.

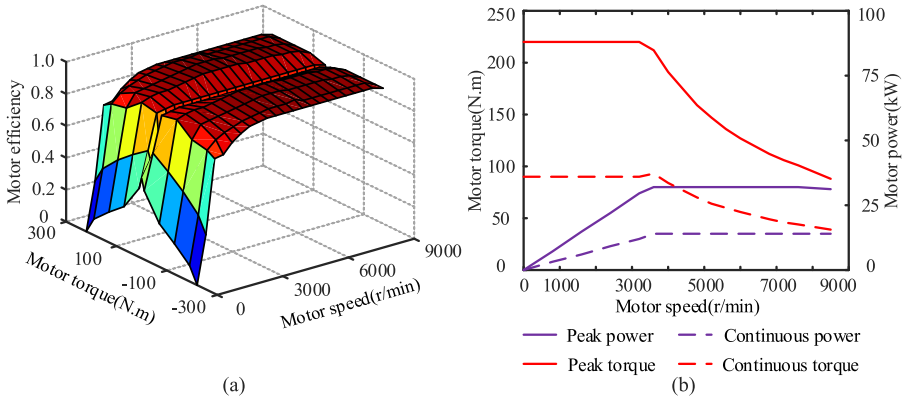

FIGURE 2. P2.5-motor characteristic model: (a) P2.5-motor efficiency model; (b) P2.5-motor characteristic diagram.

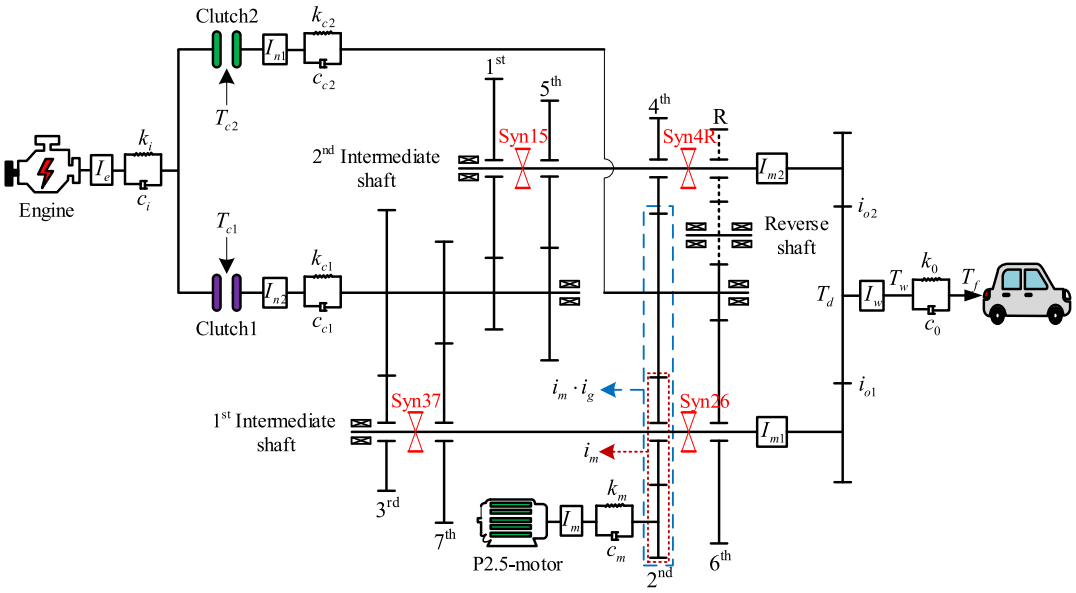

FIGURE 3. Simplified DCT system dynamics model based on the P2.5-PHPS.

III. DYNAMIC ANALYSIS AND EVALUATION INDEX

A. SIMPLIFIED KINETIC MODEL OF P2.5-PHPS

The structure of the P2.5-PHPS is novel and has rarely been subjected to dynamic analyses. According to the structural diagram of the P2.5-PHPS equipped with DCT, the DCT can be simplified as a discrete system, and a simplified dynamic model of the DCT under the P2.5-PHPS can be established, as shown in Fig. 3. With regard to the working principle and kinematics, a DCT is equivalent to using two sets of traditional manual transmissions. The first transmission connects all the odd gears, and the second transmission connects all the even gears. The output torque of the engine is transferred to different input shafts through two clutches, thereby transmitting the torque to the transmission [18], [19]. When the P2.5-motor outputs the driving torque, the clutch need not be combined, and the engine can choose to engage any clutch to output the driving torque.

The input shaft and output shaft models can be simplified to spring damper models, and the gears can be simplified to lumped mass models [20]–[22], as shown in Fig. 3.

The following assumptions are made for the model: (a) the gap between the gear and the system is ignored; (b) each module of the transmission system is embodied as a concentrated mass; and (c) the effects of secondary factors (such as clutch heat recession) are ignored.

In Fig. 3, I_e represents the moment of inertia of the engine output shaft, including the rotating parts of the engine and driving plate of C2; I_m represents the equivalent moment of inertia on the P2.5-motor output shaft, including the equivalent moments of inertia corresponding to the P2.5-motor output shaft between the P2.5-motor rotor, P2.5-motor output shaft, and 2nd gear of transmission; I_{n1} represents the driven plate damper of C2, which consists of the input shaft 2 (hollow shaft) and associated even-gear moment of inertia; I_{m1} represents the moment of inertia of the driving part of intermediate shaft 1, its associated gear, and final drive 1; I_w represents the moment of inertia from the wheel end of the vehicle and is equal to that of the output shaft; i_g represents the transmission-speed ratio; i_m represents the speed ratio from the motor to shaft 3; k_i, k_m, and k_0 represent the torsional stiffness values of the engine, motor, and wheel vibration damper, respectively; k_{c2} represents the torsional stiffness of the C2 damper; c_i, c_m, and c_0 represent the rotational viscous damping coefficients of the engine, motor, and wheel damper, respectively; c_{c2} represents the rotational viscous damping coefficient of the C2 damper; T_{c2} represents the transmitting torque of C2; and T_f represents the resistance torque of the vehicle.

B. DYNAMIC EQUATION

During the startup process of the vehicle, the torque transmitted by the power source is transmitted to the wheels through the clutch, transmission, final drive, etc. Owing to the low speed, only the rolling resistance, acceleration resistance, and slope resistance of the vehicle need to be considered. The specific vehicle dynamics expression is as follows:

$$T_f = r \cdot \left(mg \cdot \sin\theta + mgf \cdot \cos\theta + \delta m \cdot \frac{du}{dt} \right) / \eta_t, \quad (1)$$

where m represents the vehicle mass, g represents the gravitational acceleration, f is the rolling resistance coefficient, θ represents the climbing slope, r represents the wheel radius, v represents the speed, δ represents the rotation mass conversion factor of the wheel, and η_t represents the transmission efficiency.

According to the moving state of the vehicle, the startup process can be divided into two stages: (a) the vehicle remains stationary and (b) the vehicle begins to move.

In the stationary phase, the entire vehicle is subjected to the torque of the motor drive, braking torque, and resistance torque. The pure electric startup dynamic equation for the P2.5-PHPS in a stationary vehicle is as follows:

$$\begin{cases} T_m - k_m(\theta_m - \theta_1) - c_m(\omega_m - \omega_1) - T_{mg2s} = I_m \cdot \dot{\omega}_m \\ T_{mg2s} \cdot i_m - T_g - C_g^{equ} \cdot \omega_g = I_g^{equ} \cdot \dot{\omega}_g \\ T_g \cdot i_{o1} - T_w = I_w \cdot \dot{\omega}_0 \\ T_w - k_0(\theta_0 - \theta_w) + c_0(\omega_0 - \omega_w) - T_f - T_b = I_v \cdot \dot{\omega}_w \\ T_b = F_b \cdot r \end{cases} \tag{2}$$

At the beginning of the vehicle movement, the vehicle is subject to the torque of the motor drive and resistance torque, and the braking torque is zero. The pure electric startup dynamic equation for the P2.5-PHPS at the beginning of the vehicle movement is as follows:

$$\begin{cases} T_m - k_m(\theta_m - \theta_1) - c_m(\omega_m - \omega_1) - T_{mg2s} = I_m \cdot \dot{\omega}_m \\ T_{mg2s} \cdot i_m - T_g - C_g^{equ} \cdot \omega_g = I_g^{equ} \cdot \dot{\omega}_g \\ T_g \cdot i_{o1} - T_w = I_w \cdot \dot{\omega}_0 \\ T_w - k_0(\theta_0 - \theta_w) + c_0(\omega_0 - \omega_w) - T_f = I_v \cdot \dot{\omega}_w, \end{cases} \tag{3}$$

where T_m represents the P2.5-motor output torque; T_{mg2s} represents the shaft 1 output torque; ω_m represents the P2.5-motor angular speed; ω_1 represents the shaft 1 output angular speed; θ_m and θ_1 represent the angular displacements corresponding to ω_m and ω_1, respectively; i_{a1} represents the final drive speed ratio; T_g represents the shaft 3 and final drive pinion transmission torque; ω_g represents the axle 3 angular speed; T_w represents the wheel transmission torque; ω_0 represents the half-axle angular speed; ω_w represents the wheel angular speed; θ_0 and θ_w represent the angular displacements corresponding to ω_0 and ω_w, respectively; T_b represents the braking torque; and F_b represents the braking force.

In Equations (2) and (3), I_g^{equ} and C_g^{equ} are the equivalent moment of inertia and rotating viscous damping coefficient, respectively [23], [24]. The results are given by Equation (4).

$$\begin{cases} I_g^{equ} = I_s + \dfrac{i_{o1}^2}{\eta_t} \cdot I_{m2} + (I_{m1} + I_{g2}) \cdot i_{o1}^2 \cdot \eta_t \\ + I_{c2} \cdot i_{m2}^2 \cdot i_{o1}^2 \cdot \eta_t^2 + \dfrac{i_2^2 \cdot i_{o1}^2 \cdot \eta_t}{i_4^2} \cdot I_{g4} + \dfrac{i_2^2 \cdot i_{o1}^2 \cdot \eta_t}{i_6^2} \cdot I_{g6} \\ C_g^{equ} = c_s + \dfrac{i_{o1}^2}{\eta_t} \cdot c_{m2} + (c_{m1} + c_{g2}) \cdot i_{o1}^2 \cdot \eta_t \\ + c_{c2} \cdot i_{m2}^2 \cdot i_{o1}^2 \cdot \eta_t^2 + \dfrac{i_2^2 \cdot i_{o1}^2 \cdot \eta_t}{i_4^2} \\ \quad \cdot c_{g4} + \dfrac{i_2^2 \cdot i_{o1}^2 \cdot \eta_t}{i_6^2} \cdot c_{g6} \end{cases} \tag{4}$$

Here, I_s represents the moment of inertia of the output shaft, and i_2 and i_4 represent the ratios of the 2nd and 4th gears of the transmission, respectively.

The relationships among the speed of transmission input shaft 2, the intermediate shafts, the output shaft, and the P2.5-motor are as follows:

$$\omega_m = \omega_1 \cdot i_m,\ \omega_1 = \omega_{ms2g} \cdot i_2,\ \omega_{ms2g} = \omega_g \cdot i_{o1}. \tag{5}$$

Here, i_m represents the reduction ratio from the P2.5-motor output shaft to the input shaft of the transmission.

E_g^{equ} is the magnification factor of the torque transferred by C2 and corresponds to the transmission output shaft, as follows:

$$E_g^{equ} = i_m \cdot i_2 \cdot i_{o1} \cdot \eta^3. \tag{6}$$

C. EVALUATION INDEX FOR STARTUP PROCESS

In the startup process of a vehicle, most of the mechanical energy output by the power source is converted into kinetic energy, for example, into the sliding work of the driving and driven plates of the clutch. The research object of this study is a P2.5-PHPS, in which the P2.5-motor is placed behind the clutch. The torque of the power source does not pass through the clutch during pure electric startup; thus, it is unnecessary to consider the friction work of the clutch.

The vehicle jerk of the vehicle affects the driving comfort, and sliding backward during vehicle startup can seriously affect the safety of the driver and passengers [25], [26]. In summary, the vehicle jerk degree and backward sliding distance are used to evaluate the startup quality of the pure electric startup process.

1) VEHICLE JERK

The vehicle jerk degree represents the change rate of the vehicle's longitudinal acceleration [27]. The magnitude of this vehicle jerk can be expressed as follows:

$$j = \frac{dv^2}{dt} = \frac{da}{dt} = \frac{i_m \cdot i_2 \cdot i_{o1}}{\delta \cdot m \cdot r} \cdot \eta^3 \cdot \frac{dT_m}{dt}, \tag{7}$$

where δ is the coefficient of the revolving mass changes, i_2 represents the ratio of the 2nd gear of the DCT, and η_v represents the total efficiency of the vehicle transmission system. Regarding the vehicle jerk degree, the recommended value in Germany is 10 m/s^3.

2) DISTANCE OF SLIDING BACKWARD

The "distance of sliding backward" refers to the distance by which the vehicle slides backward when it starts on an incline. Generally, to ensure the safety of the driver and the surroundings of the vehicle, the distance of sliding backward should be minimized.

IV. TYPICAL CONTROL STRATEGY AND ANALYSIS

A. TYPICAL CONTROL PROBLEMS

In the P2.5-PHPS, the P2.5-motor is placed behind the clutch. The clutch does not need to be employed during pure electric startup, similar to the case of mainstream pure EV configurations.

The vehicle startup process can be divided into two stages: (a) the stationary stage and (b) the movement stage.

When the vehicle is in the stationary stage, its parameters cannot be determined directly and quickly using the dynamic equation; they can only be approximated via slope estimation after motion. Therefore, the motor output torque is difficult to control during the period from the beginning of vehicle movement to the slope estimation. This can easily cause problems such as sliding backward, evident catapulting, and vehicle jerk, directly affecting the startup quality.

B. UPHILL STARTUP PROCESS

During a pure electric uphill startup, the vehicle is subjected to motor torque, brake torque, slope, and vehicle mass. Fig. 4 presents a torque variation diagram for the traditional pure electric uphill startup process, where T_{bmax} represents the maximum braking torque, T_{max_α} represents the minimum anti-sliding slope torque corresponding to the current vehicle slope value, and T_f represents the sum of the resistance torque at the wheel end of the vehicle.

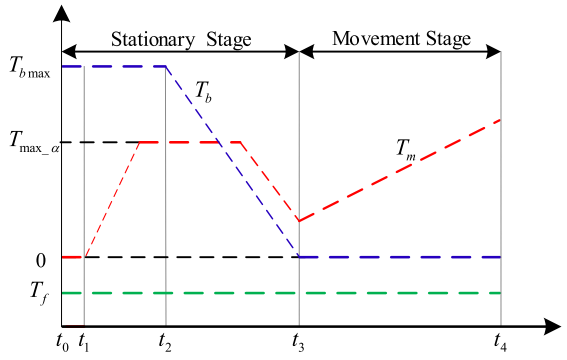

FIGURE 4. Torque variation for a typical electric uphill startup process.

t_0–t_1: The vehicle is in an uphill parked state; the driver steps on the brake and clutch pedals, puts the transmission lever in position D, and prepares to start driving uphill.

t_1–t_2: In the control strategy for a typical pure electric startup, according to the maximum allowable slope, the initial anti-slide backward torque is set and maintained. At this time, the driver does not release the brake pedal, and the braking torque does not change.

t_2–t_3: The brake pedal begins to relax, the brake torque decreases, and the initial anti-slide backward torque is maintained. At this stage, to ensure a smooth start, it is necessary to adjust the change rate of the driving torque according to the change rate of the braking torque; that is, the driving torque of the motor should be equal to the sum of the braking and resistance torques.

t_3–t_4: When the driver releases the brake pedal and the brake torque drops to zero, the motor torque only needs to overcome the resistance torque. According to the driver's startup intention, the motor outputs the driving torque and its change rate under the limit of the vehicle jerk degree and other indicators, completing the uphill startup process.

C. DOWNHILL STARTUP PROCESS

The difference between the pure electric downhill and uphill startup processes is that in the former, the vehicle receives torque (such as that due to slope and vehicle mass) as part of the power for vehicle movement, rather than as resistance. The torque variation diagram for a typical pure electric downhill startup process is shown in Fig. 5.

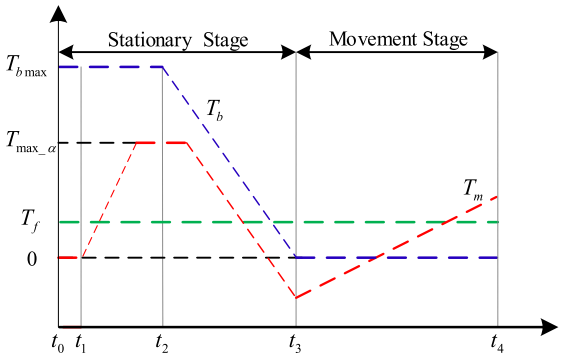

FIGURE 5. Torque variation for a typical electric downhill startup process.

t_0–t_1: The vehicle is in the downhill parked state; the driver steps on the brake and clutch pedals, puts the transmission lever in D, and prepares to start driving downhill.

t_1–t_2: In the control strategy for a typical pure electric startup, according to the maximum allowable slope, the initial anti-slide backward torque is set and remains as such. At this time, the driver does not release the brake pedal, and the braking torque does not change.

t_2–t_3: The brake pedal is relaxed, the brake torque decreases, and the initial anti-slide backward torque is maintained. At this stage, to ensure a smooth start, it is necessary to adjust the change rate of the driving torque according to the change rate of the braking torque; that is, the sum of the motor torque and the torque due to the slope and vehicle mass should be equal to the brake torque. When the motor torque is less than zero, the vehicle is in the brake power generation state.

t_3–t_4: When the driver releases the brake pedal and the brake torque drops to zero, the motor torque starts to decrease, and the motor outputs the driving torque at the later stage to complete the downhill startup process.

D. TYPICAL CONTROL STRATEGY PROBLEMS

According to the analysis of the different stages of the pure electric startup process, together with the typical control strategies of a startup process, the following observations are made.

1) To ensure that the vehicle does not slide backward during the startup process, the initial anti-slide backward torque is set according to the maximum allowable slope in the early stationary stage of the vehicle. This strategy can effectively prevent the vehicle from sliding backward before it starts to move uphill. However, an excessive initial torque can easily

cause evident catapults and vehicle jerk during startups on small uphill and downhill slopes, respectively.

2) The initial torque is set according to the maximum allowable slope. Under the assumption that the driver's startup intention is considered, the motor torque will be adjusted accordingly, based on the typical startup strategy. When the slope changes, the motor torque cannot effectively adapt to the driver's real startup demand.

V. CONTROL STRATEGY

A. FRAMEWORK OF STARTUP PROCESS

In view of the shortcomings of typical control strategies related to the pure electric startup process, a pure electric startup control strategy for a P2.5-PHPS equipped with a DCT is proposed, which is based on the slope memory and startup intention identification.

The pure electric startup control strategy considered in this study is divided into four parts: **1)** slope memory estimation; **2)** initial torque setting based on slope memory; **3)** startup intention recognition based on driver operations; **4)** torque compensation based on the ramp slope and the driver's startup intention.

The control-strategy framework for the pure electric startup process is shown in Fig. 6.

B. INITIAL TORQUE SETTING

According to the latest parking time before startup, the value of the slope is calculated and stored in the controller. When the vehicle starts, the value of the slope is read and called, and the initial startup anti-slide backward torque is formulated for the adaptive slope.

$$\begin{cases} F_{t\max\_\alpha} = mgf \cdot \cos\alpha_{\max} + mg \cdot \sin\alpha_{\max} \\ F_b = \dfrac{\beta_b \cdot T_{b\_\max}}{r} \end{cases} \tag{8}$$

Here, α represents the slope, β_b represents the brake-pedal opening, F_{b_max} represents the maximum braking force, F_b represents the braking force, and T_{b_max} represents the maximum braking torque.

The equilibrium equation for the critical point of the vehicle motion is as follows:

$$F_t = F_b + mgf \cdot \cos\alpha + mg \cdot \sin\alpha. \tag{9}$$

The slope angle ϑ is determined using Equations (8) and (9), as follows:

$$\begin{cases} \alpha = \arcsin \dfrac{F_{t\max\_\alpha} - F_b}{mg \cdot \sqrt{1+f^2}} - \arctan f \\ \vartheta = \tan\alpha \end{cases} \tag{10}$$

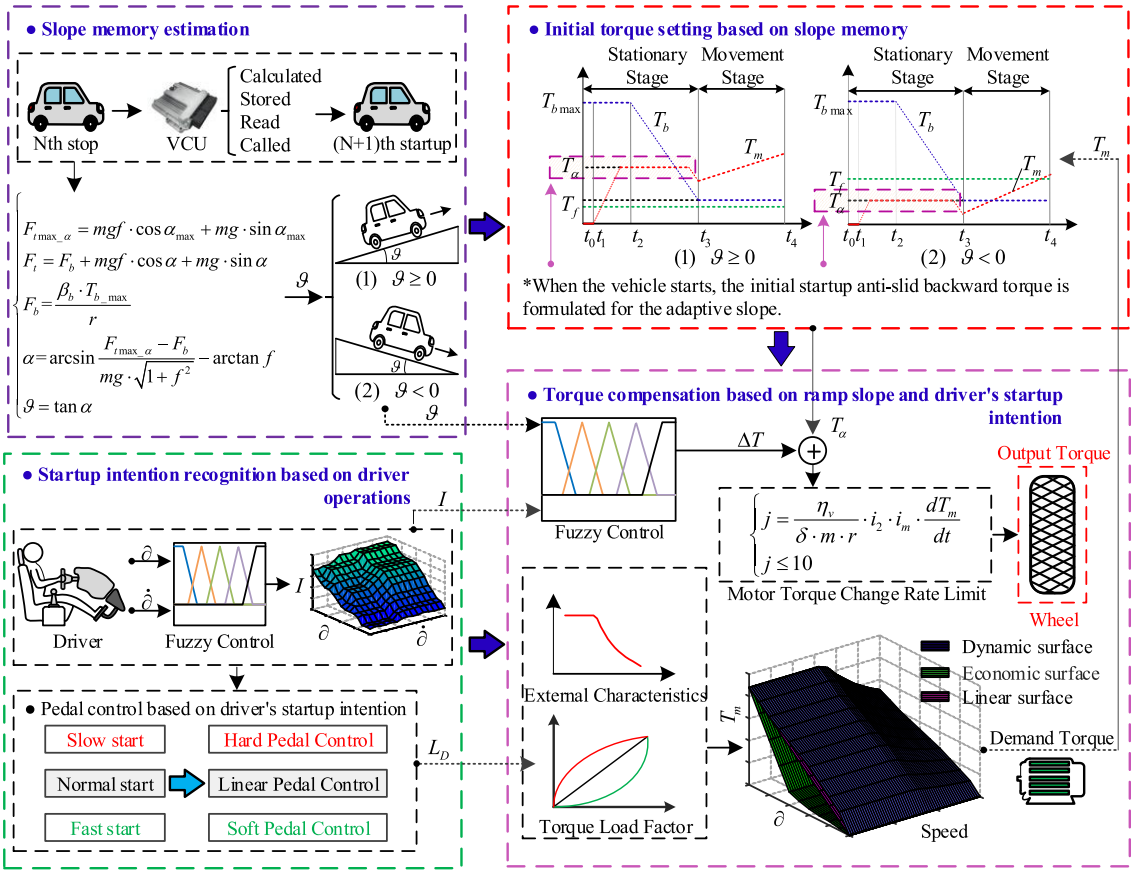

FIGURE 6. Control-strategy framework for the pure electric startup process.

Therefore, the value of the startup initial driving output torque corresponds to the read climbing angle. The initial driving torque value of the uphill output corresponds to the slope angle, whereas the initial driving torque value of the downhill output is zero. This approach can effectively prevent backward sliding when the vehicle is started on an uphill slope and avoid catapulting and evident vehicle jerk during startup on small uphill and downhill slopes, respectively.

C. STARTUP INTENTION RECOGNITION

An accurate driver model is important for startup quality. In this study, a multi-layer fuzzy control strategy is used to simulate the driver's startup experience and is transformed into fuzzy control logic rules to accurately identify the driver's intention [28]–[31].

Suppose that the fuzzy language for an accelerator pedal opening (α) is {very small (VS), small (S), medium (M), big (B), very big (VB)}, with the basic universe of [0, 1]; the fuzzy language for the accelerator pedal opening change rate ($\dot{\alpha}$) is {negative big (NB), negative middle (NM), negative small (NS), zero (Z), positive small (PS), positive middle (PM), positive big (PB)}, with the basic universe of [−1, 1]; and the fuzzy language for the startup intention (I) is {very small (VS), small (S), medium (M), big (B), very big (VB)}, with the basic universe of [0, 1].

A fuzzy control strategy diagram for the driver's startup intention (considering the driver's operation) is shown in Fig. 7. According to the membership function of the inputs and outputs of the fuzzy control, as well as the fuzzy control rules, the fuzzy control surface is obtained.

D. TORQUE COMPENSATION

According to the driver's operations, the driver's startup intention can be classified as one of three types: slow start, normal start, and fast start. The accelerator pedal is classified into three types: hard pedal, linear pedal, and soft pedal. The hard pedal reflects the dynamic performance of the entire vehicle, but the handling stability is poor under low loads. The soft pedal enhances the economic performance of the vehicle, but the acceleration is low under a strong startup intention; the control effect of the linear pedal is intermediate. According to the three different startup intentions, a control strategy is formulated for the accelerator pedal: the hard pedal enables a fast start, the soft pedal enables a slow start, and the linear pedal enables a normal startup. This approach better reflects the startup needs of the drivers.

The dynamic demand of the vehicle can be expressed using the climbing slope of the vehicle. Therefore, different dynamic curves of the vehicle are calculated according to the power demands under different climbing slopes. The vehicle's economy is expressed through the driving motor working in the high-efficiency range; thus, the vehicle economy curve is calculated in the high-efficiency range of the driving motor. The different driving torques corresponding to the motor speeds under different accelerator pedal opening degrees are calculated. The relationships among the three variables were determined using the interpolation method and are presented in Fig. 8.

To ensure that the vehicular states under different startup conditions can adequately follow the driver's startup demands, the identified driver's intention is combined with

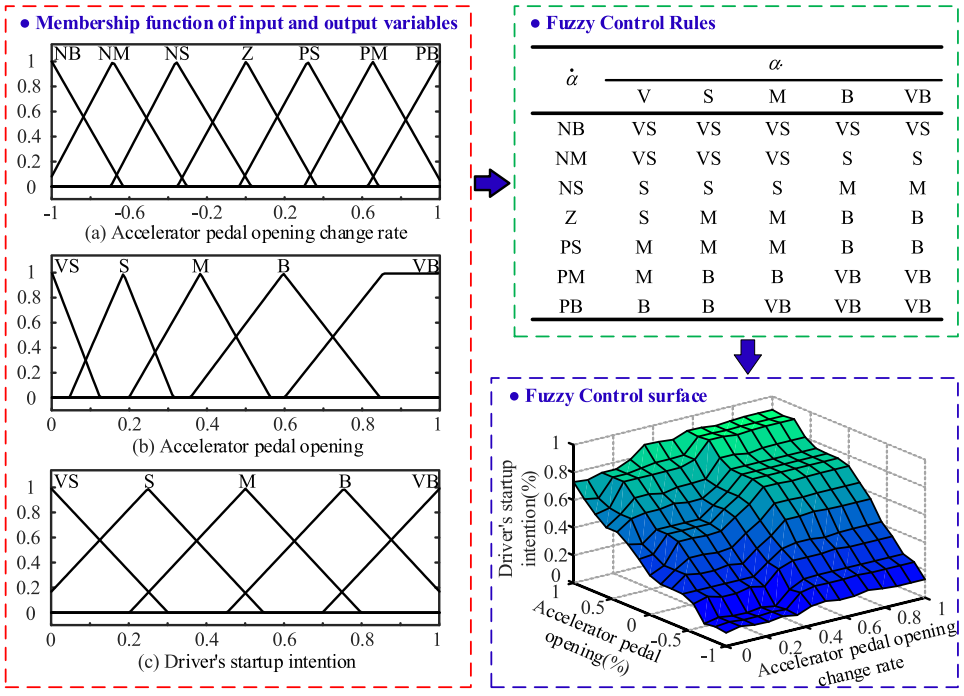

FIGURE 7. Fuzzy control strategy diagram of the driver's startup intention.

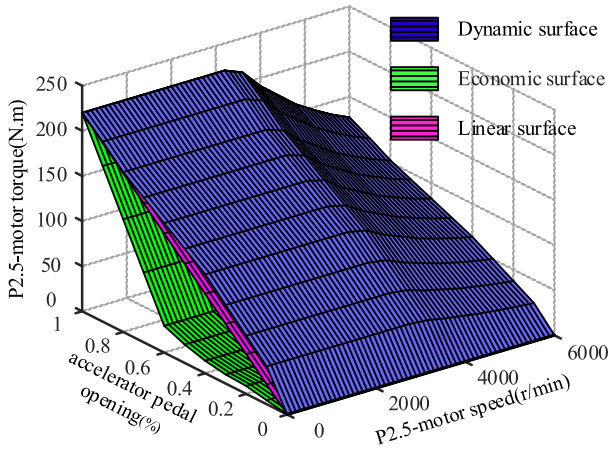

FIGURE 8. Characteristic surface of the pedal control torque.

the slope to compensate for the torque during the startup process under different startup conditions. A sudden change in the driving torque significantly affects the smoothness of the vehicle startup. Therefore, the maximum vehicle jerk degree should be considered in the maximum compensation torque [31].

$$\begin{cases} j = \dfrac{dv^2}{dt} = \dfrac{da}{dt} = \dfrac{\eta_v}{\delta \cdot m \cdot r} \cdot i_2 \cdot i_m \cdot \dfrac{dT_m}{dt} \\ j \le 10 \end{cases} \tag{11}$$

Therefore, to ensure ride comfort, the torque change rate of the P2.5-motor should satisfy

$$dT_m / dt_{\max} \le j_{amx} \cdot \frac{\delta \cdot m \cdot r}{i_2 \cdot i_m \cdot \eta_v}. \tag{12}$$

If the technical requirements of the P2.5-motor are considered, the theoretical response time is approximately 20 ms [33]. Combined with the specific parameters of the research object in this study, the maximum torque compensation of the P2.5-motor within the motor response time under the maximum vehicle jerk limit is approximately 15 N·m. According to this result, a torque compensation strategy combining the ramp data and the driver's startup intention is developed.

Suppose that the fuzzy language for the driver's startup intention (I) is {very small (VS), small (S), medium (M), big (B), very big (VB)}, with the basic universe of [0, 1]; the fuzzy language of the climbing angle (I) is {very small (VS), small (S), medium (M), big (B), very big (VB)}, with the basic universe of [0, 1]; and the fuzzy language for torque compensation (ΔT) is {very small (VS), small (S), medium (M), big (B), very big (VB)}, with the basic universe of [0, 1].

The fuzzy control strategy diagram for torque compensation combining the ramp data and the driver's startup intention is shown in Fig. 9. According to the membership function of the inputs and outputs of the fuzzy control and fuzzy control rules, a fuzzy control surface is obtained.

VI. MODELING AND SIMULATION ANALYSIS

According to the analysis of the configuration and startup process, together with the corresponding startup control strategy, a pure electric startup model for a P2.5-PHPS equipped with a DCT was established and simulated.

To ensure the accuracy of the control algorithms (e.g., torque compensation) under different startup intentions,

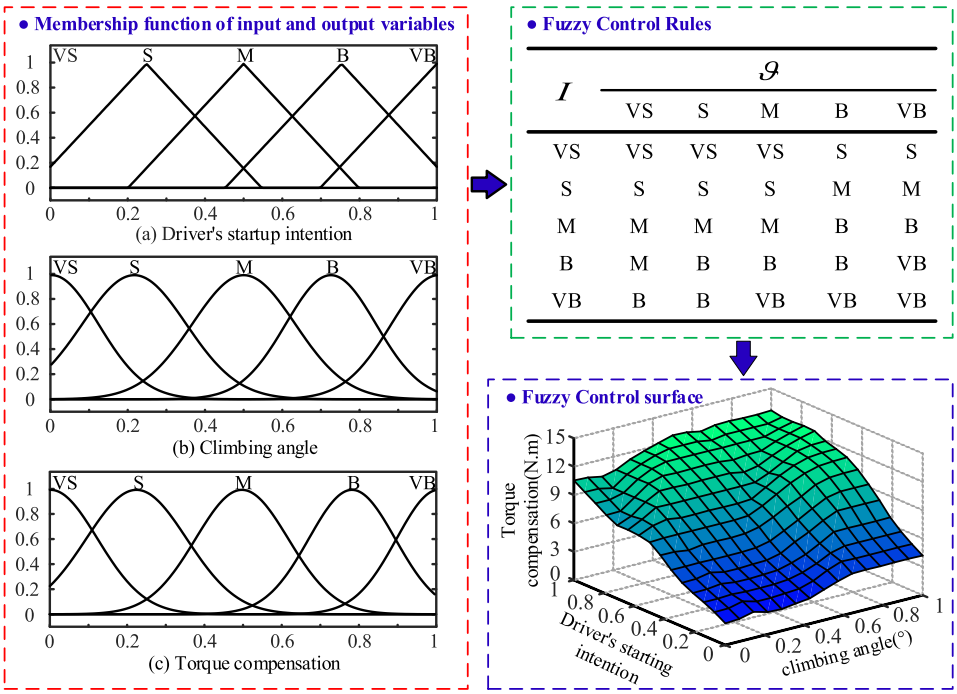

FIGURE 9. Fuzzy control strategy diagram for torque compensation.

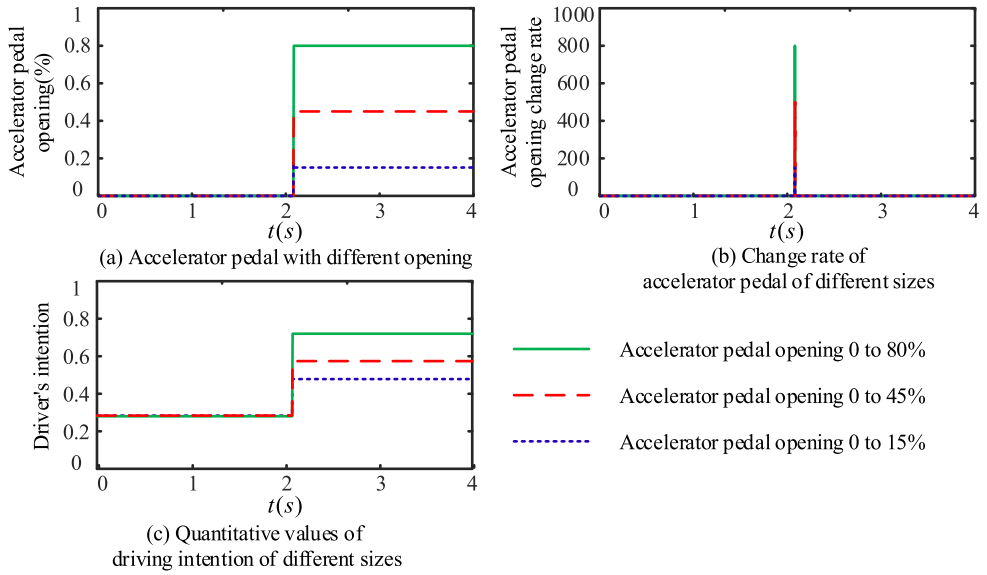

FIGURE 10. Simulation of driver's startup intention verification.

it was necessary to verify the recognition of the drivers' startup intentions under different operations. By applying step signals of 0% to 15%, 0% to 45%, and 0% to 80% to the accelerator pedal opening, the change rate of the accelerator pedal opening and driver's startup intention curves under different step signals were obtained, as shown in Figs. 10(b) and 10(c), respectively. As shown in Fig. 10, when the accelerator pedal opening changed in positive gradient steps, the rate of change of the accelerator pedal opening and the quantitative value of the driver's startup intention increased. The results indicate that the driver's startup intention strategy can effectively track the changing trend of the accelerator pedal opening and its change rate, providing a basis for accurate torque compensation in combination with the road condition information.

To compare and analyze the startup performance and effectiveness of the control strategy under different startup intentions and slopes, uphill and downhill startup conditions were simulated and verified.

1) The maximum opening of the accelerator pedal was set as 15%, the change rate of the fixed accelerator pedal opening was 0.05, and the climbing angle was 5%. The simulation results for the startup process are shown in Fig. 11.

A comparison of the motor-torque simulation results based on this control strategy and a traditional typical control strategy is shown in Fig. 11. As indicated by Fig. 11(a), in the typical startup control strategy for 0–0.4 s, the initial startup torque was applied, and the maximum initial slide backward torque was reached at 0.4 s. The maximum vehicle jerk was approximately 9.83 m/s^3. In the proposed startup control strategy, the slope value calculated and stored in the controller at the last parking time was read during the startup, and the initial startup anti-slide backward torque of the adaptive slope was formulated. It reached a maximum value of approximately 70 N·m at approximately 0.2 s. At approximately 1.47 s, the torque change rate of the P2.5-motor corresponded to the change rate of the braking torque, and the P2.5-motor was in the driving state. At approximately 1.50 s, the braking torque was zero, and the output torque increased. A comparison diagram of the distance of sliding backward for the startup process is presented in Fig. 11(d). As shown, during an uphill startup, the backward sliding can be effectively prevented using both the typical method and the proposed method. A speed comparison diagram for the startup process is presented in Fig. 11(b). As shown, the torque compensation strategy considering the combination of the ramp and the driver's startup intention increased more quickly after the vehicle started to move and better reflected the driver's startup demand. A vehicle jerk comparison diagram for the startup process is shown in Fig. 11(c). As shown, the maximum vehicle jerk of the entire startup process was approximately 7.31 m/s^3.

Based on the comparative analysis and the startup control strategy, backward sliding can be effectively prevented during an uphill startup. Moreover, the slope resistance moment is small when the startup is conducted on a small uphill slope, and the new method can prevent catapulting. The maximum vehicle jerk of the entire startup process was 7.31 m/s^3—an effective reduction of 25.4%.

2) The maximum opening of the accelerator pedal was set as 15%, the change rate of the fixed accelerator pedal opening was 0.10, and the climbing angle was 15%. The simulation results are shown in Fig. 12.

A comparison of the motor-torque simulation results for the proposed control strategy and a typical control strategy is presented in Fig. 12. As shown in Fig. 12(a), for the typical startup control strategy, the initial startup torque was applied from 0 to 0.4 s, and the maximum initial startup torque

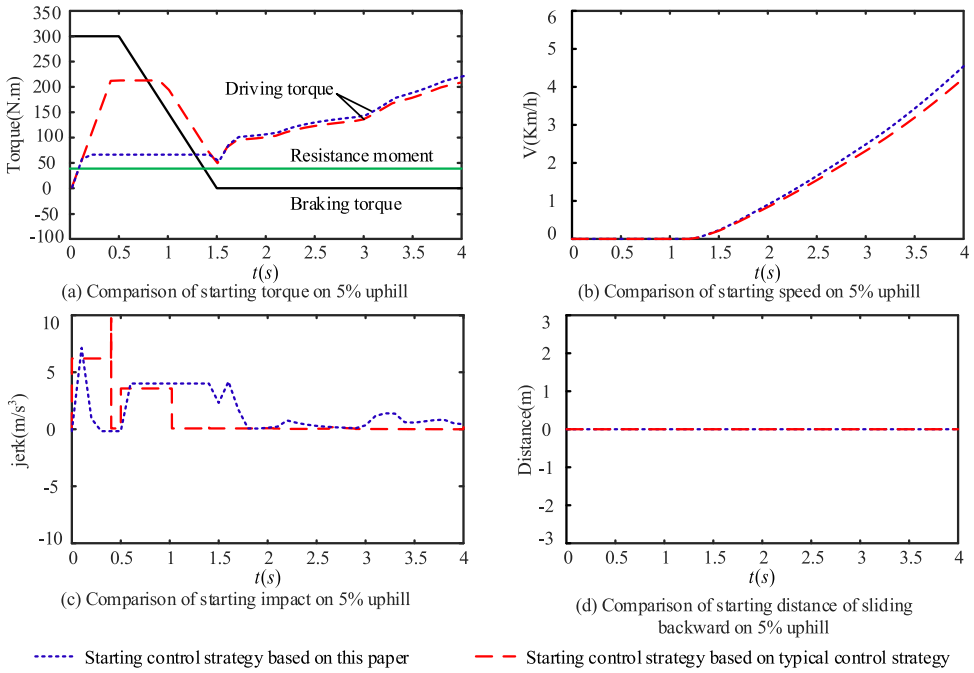

FIGURE 11. Comparison of the simulation results for uphill startup on a small slope.

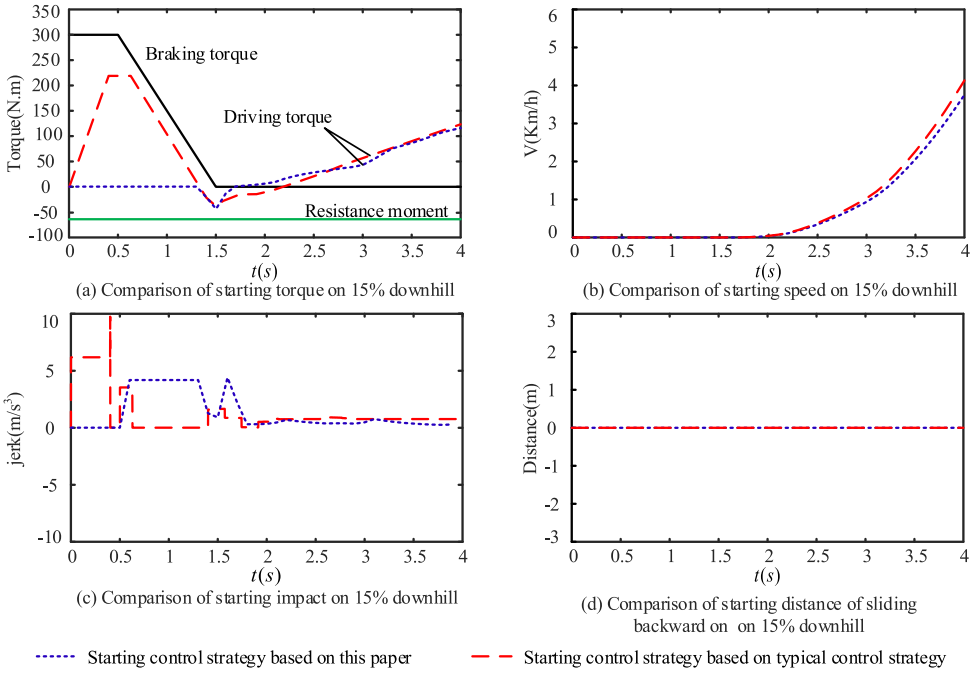

FIGURE 12. Comparison of the simulation results for downhill startup on a medium slope.

value was reached at 0.4 s. The maximum vehicle jerk was approximately 9.83 m/s^3. For the proposed startup control strategy, the initial startup anti-slide backward torque for the adaptive slope was zero (determined by reading the value calculated and stored in the controller at the last parking time). At approximately 1.4 s, the torque change rate of the P2.5-motor corresponded to the change rate of the braking torque. At this time, the P2.5-motor was in the braking power generation state. When the braking torque became zero at approximately 1.5 s, the braking power generation torque of the P2.5-motor decreased, and the driving torque was gradually output. A comparison diagram of the distance of sliding

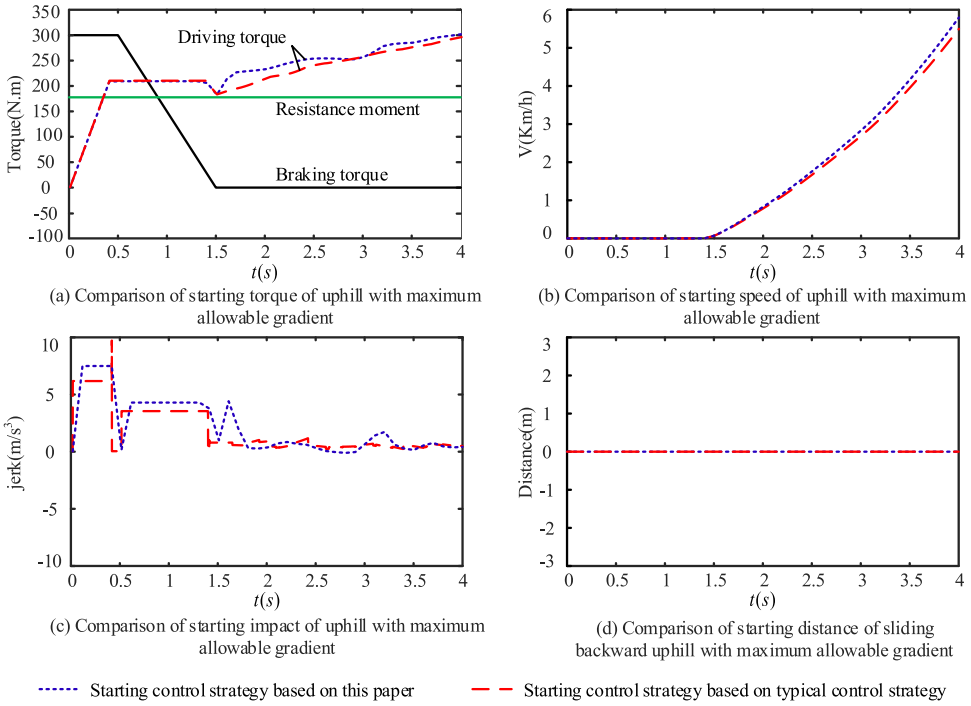

FIGURE 13. Comparison of the simulation results for uphill startup on the maximum allowable slope.

backward for the startup process is presented in Fig. 12(d). The backward sliding can be effectively prevented during a downhill startup using both the typical method and the proposed method. The speeds of the startup processes were compared, as shown in Fig. 12(b). In the torque compensation strategy considering the ramp and the driver's startup intention after the vehicle started to move, the speed increased more slowly, better reflecting the driver's startup demand. A vehicle jerk comparison diagram for the startup process is presented in Fig. 12(c). As shown, the maximum vehicle jerk of the entire startup process was approximately 4.18 m/s^3.

Compared with the typical startup strategy, the proposed startup control strategy better reflected the advantages of the vehicle and provided better startup quality in a downhill startup process. The maximum vehicle jerk of the entire startup process was 4.18 m/s^3—an effective reduction of 57.5%.

3) The maximum opening of the accelerator pedal was set as 80%, the rate of change of the fixed accelerator pedal opening was 0.11, and the climbing angle was 25%. The simulation results are shown in Fig. 13.

A comparison of the motor-torque simulation results for the proposed control strategy and a typical control strategy is shown in Fig. 13. As shown in Fig. 13(a), for the typical startup control strategy, the initial startup torque was applied from 0 to 0.4 s, and the maximum initial startup torque value was reached at 0.4 s. The maximum vehicle jerk was approximately 9.83 m/s^3. For the proposed startup control strategy, the slope value calculated and stored in the controller at the last parking time was read during startup, and the initial startup anti-slide backward torque of the adaptive slope was determined. It reached a maximum value of approximately 0.5 s, that is, approximately 220 N·m. At approximately 1.47 s, the torque change rate of the P2.5-motor corresponded to the change rate of the braking torque, and the P2.5-motor was in the driving state. At approximately 1.50 s, the braking torque was zero, and the output torque increased. A comparison diagram of the distance of sliding backward for the startup process is presented in Fig. 13(d). The backward sliding can be effectively prevented during an uphill startup using both the typical method and the proposed method. A speed comparison diagram for the startup process is presented in Fig. 13(b). As shown, the torque compensation strategy combining the ramp and the driver's startup intention increased more quickly after the vehicle started to move and better reflected the driver's startup demand. A vehicle jerk comparison diagram for the startup process is shown in Fig. 13(c). As shown, the maximum vehicle jerk of the entire startup process was approximately 7.51 m/s^3.

In contrast with the typical startup strategy, the maximum initial torque corresponding to the maximum climbing angle is applied in the stationary stage of the vehicle. The new method can effectively reduce the vehicle jerk by limiting the change rate of the driving torque. The maximum vehicle jerk degree was 7.51 m/s^3—an effective reduction of 23.6%.

VII. CONCLUSION

1) For a P2.5-PHPS equipped with a DCT, control strategies for a typical pure electric startup process are analyzed in several stages. The current pure electric startup strategy,

which employs a slope-memory strategy to set the initial anti-slide backward torque, is proposed to estimate and store the slope during the vehicle movement before parking. This can not only prevent the vehicle from sliding backward when it starts on an uphill slope but also avoid catapulting and evident vehicle jerk when it starts on small uphill and downhill slopes, respectively.

2) Targeting the shortcomings of a typical pure electric startup control strategy, a pure electric startup control strategy based on slope memory and recognition of the driver's startup intention is proposed. According to the last parking time before startup, the slope value is calculated and stored in the controller. When the vehicle starts the next time, the slope value is read, and the startup initial anti-slide backward torque for the adaptive slope is formulated. Simultaneously, with the vehicle jerk degree regarded as the target (and with consideration of the driver's startup intention and the slope value), an adaptive compensation torque is provided to prevent catapulting and evident vehicle jerk.

3) Simulation results indicated that the driver's operation can be accurately identified by establishing a driver's startup intention strategy and that a pure electric startup control strategy based on slope memory and recognition of the driver's startup intention can prevent a vehicle from sliding backward and catapulting. Such a strategy can also reduce the vehicle jerk and provide better startup quality than the typical startup control strategy.

4) This study was based on a P2.5-PHPS equipped with a DCT. For other hybrid power systems, similar studies can be conducted with consideration of the driver's startup intention and the slope value for evaluating the adaptability of this method to different vehicles.

REFERENCES

[1] J. DeCarolis, H. Daly, P. Dodds, I. Keppo, F. Li, W. McDowall, S. Pye, N. Strachan, E. Trutnevyte, W. Usher, M. Winning, S. Yeh, and M. Zeyringer, "Formalizing best practice for energy system optimization modelling," *Appl. Energy*, vol. 194, pp. 184–198, May 2017.

[2] Y. Yang, Y. Zhang, J. Tian, and T. Li, "Adaptive real-time optimal energy management strategy for extender range electric vehicle," *Energy*, vol. 197, Apr. 2020, Art. no. 117237.

[3] J. Hong, Z. Wang, T. Zhang, H. Yin, H. Zhang, W. Huo, Y. Zhang, and Y. Li, "Research on integration simulation and balance control of a novel load isolated pure electric driving system," *Energy*, vol. 189, Dec. 2019, Art. no. 116220.

[4] M. Kulkarni, T. Shim, and Y. Zhang, "Shift dynamics and control of dual-clutch transmissions," *Mechanism Mach. Theory*, vol. 42, no. 2, pp. 168–182, Feb. 2007.

[5] M. Goetz, M. C. Levesley, and D. A. Crolla, "Dynamics and control of gearshifts on twin-clutch transmissions," *Proc. Inst. Mech. Eng., D, J. Automobile Eng.*, vol. 219, no. 8, pp. 951–963, Aug. 2005.

[6] R. Bao, V. Avila, and J. Baxter, "Effect of 48 V mild hybrid system layout on powertrain system efficiency and its potential of fuel economy improvement," SAE Tech. Papers 2017-01-1175, 2017, doi: 10.4271/2017-01-1175.

[7] X. Xu, Y. Liang, M. Jordan, P. Tenberge, and P. Dong, "Optimized control of engine start assisted by the disconnect clutch in a P2 hybrid automatic transmission," *Mech. Syst. Signal Process.*, vol. 124, pp. 313–329, Jun. 2019.

[8] J. Ning, G. Zhu, and B. Qu, "Development of a engine start control method for P2 hybrid vehicles in launch situation," *IFAC-PapersOnLine*, vol. 51, no. 31, pp. 7–10, 2018.

[9] G. Tao, M. Wu, and F. Meng, "Online performance evaluation of a heavy-duty automatic transmission launching process," *Mechatronics*, vol. 38, pp. 143–150, Sep. 2016.

[10] X. Wang, L. Li, and C. Yang, "Hierarchical control of dry clutch for engine-start process in a parallel hybrid electric vehicle," *IEEE Trans. Transport. Electrific.*, vol. 2, no. 2, pp. 231–243, Jun. 2016.

[11] H. Chen, Y. Wan, D. Jin, S. Zheng, and X. Lian, "Adaptive launching control strategy of in-wheel motor driven vehicle," in *Proc. 37th Chin. Control Conf. (CCC)*, Jul. 2018, pp. 2694–2699.

[12] M. Wu, "Sliding mode control for optimal torque transmission of dry dual clutch assembly of a two-speed electric vehicle during launch," *J. Phys., Conf. Ser.*, vol. 1314, Oct. 2019, Art. no. 012125.

[13] L. Chu, C. Guo, P. Z. Zhang, Z. C. Fu, and Y. J. Zhang, "Study on control strategy for electric starting up of pure electric vehicle," *Appl. Mech. Mater.*, vol. 721, pp. 313–316, Dec. 2014.

[14] C. Yang, J. Song, L. Li, S. Li, and D. Cao, "Economical launching and accelerating control strategy for a single-shaft parallel hybrid electric bus," *Mech. Syst. Signal Process.*, vols. 76–77, pp. 649–664, Aug. 2016.

[15] M.-S. Kim, B.-J. Kim, C.-I. Kim, M.-H. So, G.-S. Lee, and J.-H. Lim, "Vehicle dynamics and road slope estimation based on cascade extended Kalman filter," in *Proc. Int. Conf. Inf. Commun. Technol. Robot. (ICT-ROBOT)*, Sep. 2018, pp. 1–4.

[16] K. Jiang, A. C. Victorino, and A. Charara, "Real-time estimation of vehicle's lateral dynamics at inclined road employing extended Kalman filter," in *Proc. IEEE 11th Conf. Ind. Electron. Appl. (ICIEA)*, Jun. 2016, pp. 2360–2365.

[17] J. J. Hu, Y. Ji, and R. Du, "Control strategy for starting and acceleration of pure electric vehicle," *J. Appl. Sci.*, vol. 13, no. 22, pp. 5356–5362, Nov. 2013.

[18] E. Galvagno, M. Velardocchia, and A. Vigliani, "Dynamic and kinematic model of a dual clutch transmission," *Mechanism Mach. Theory*, vol. 46, no. 6, pp. 794–805, Jun. 2011.

[19] Y. Liu, D. Qin, H. Jiang, and Y. Zhang, "A systematic model for dynamics and control of dual clutch transmissions," *J. Mech. Des.*, vol. 131, no. 6, Jun. 2009, Art. no. 061012.

[20] J. Oh, S. B. Choi, Y. J. Chang, and J. S. Eo, "Engine clutch torque estimation for parallel-type hybrid electric vehicles," *Int. J. Automot. Technol.*, vol. 18, no. 1, pp. 125–135, Feb. 2017.

[21] J. J. Oh, S. B. Choi, and J. Kim, "Driveline modeling and estimation of individual clutch torque during gear shifts for dual clutch transmission," *Mechatronics*, vol. 24, no. 5, pp. 449–463, Aug. 2014.

[22] G. Lucente, M. Montanari, and C. Rossi, "Modelling of an automated manual transmission system," *Mechatronics*, vol. 17, nos. 2–3, pp. 73–91, Mar. 2007.

[23] Z. Zhao, X. Li, L. He, C. Wu, and J. K. Hedrick, "Estimation of torques transmitted by twin-clutch of dry dual-clutch transmission during vehicle's launching process," *IEEE Trans. Veh. Technol.*, vol. 66, no. 6, pp. 4727–4741, Jun. 2017.

[24] Z. G. Zhao, H. J. Chen, Z. X. Zhen, and Y. Y. Yang, "Optimal torque coordinating control of the launching with twin clutches simultaneously involved for dry dual-clutch transmission," *Vehicle Syst. Dyn.*, vol. 52, no. 6, pp. 776–801, Jun. 2014.

[25] N. Rauh, T. Franke, and J. F. Krems, "Understanding the impact of electric vehicle driving experience on range anxiety," *Hum. Factors*, vol. 57, no. 1, pp. 177–187, 2014.

[26] G. Jiang, Y. Lin, D. Qin, and M. Hu, "Torque coordination control strategy in engine starting process for a single motor hybrid electric vehicle," *Int. J. Electric Hybrid Vehicles*, vol. 10, no. 2, pp. 177–196, 2018.

[27] L. Wang, S. Zhang, X. Wang, and Y. Zhang, "Research on vehicle automatically tracking mechanism in VANET," *Int. J. Distrib. Sensor Netw.*, vol. 9, no. 8, Aug. 2013, Art. no. 592129.

[28] G. Li and J. Hu, "Modeling and analysis of shift schedule for automatic transmission vehicle based on fuzzy neural network," in *Proc. 8th World Congr. Intell. Control Automat.*, Jul. 2010, pp. 4839–4844.

[29] J. Wu, C.-H. Zhang, and N.-X. Cui, "Fuzzy energy management strategy for a hybrid electric vehicle based on driving cycle recognition," *Int. J. Automot. Technol.*, vol. 13, no. 7, pp. 1159–1167, Dec. 2012.

[30] S. Wang, Y. Liu, Z. Wang, P. Dong, Y. Cheng, X. Xu, and P. Tenberge, "Adaptive fuzzy iterative control strategy for the wet-clutch filling of automatic transmission," *Mech. Syst. Signal Process.*, vol. 130, pp. 164–182, Sep. 2019.

[31] P. Dong, S. Wu, W. Guo, X. Xu, S. Wang, and Y. Liu, "Coordinated clutch slip control for the engine start of vehicles with P2-hybrid automatic transmissions," *Mechanism Mach. Theory*, vol. 153, Nov. 2020, Art. no. 103899.
[32] K. Bayar, J. Wang, and G. Rizzoni, "Development of a vehicle stability control strategy for a hybrid electric vehicle equipped with axle motors," *Proc. Inst. Mech. Eng., D, J. Automobile Eng.*, vol. 226, no. 6, pp. 795–814, Jun. 2012.
[33] H. Mesloub, R. Boumaaraf, M. T. Benchouia, A. Goléa, N. Goléa, and K. Srairi, "Comparative study of conventional DTC and DTC_SVM based control of PMSM motor—Simulation and experimental results," *Math. Comput. Simul.*, vol. 167, pp. 296–307, Jan. 2020.

YONG LUO received the B.S. and Ph.D. degrees in automotive engineering from Chongqing University, Chongqing, China, in 2005 and 2010, respectively. He is currently an Associate Professor with the Chongqing University of Technology. He has led more than ten research projects and published more than 20 research journal articles. His main research interests include vehicle power transmission and its integrated control. His research interests include the matching, simulation, and testing of power transmission systems of automatic transmission, electric vehicles, and hybrid electric vehicles.

YONGHENG WEI is currently pursuing the master's degree with the Chongqing University of Technology, Chongqing, China. His main research interests include the optimization and control of plug-in hybrid electric vehicles and the control of vehicle automatic transmission systems.

YINGZHE KAN received the B.S. degree in automotive engineering from the Chongqing University of Technology, Chongqing, China, in 2017. He is currently pursuing the Ph.D. degree with Chongqing University, Chongqing. His main research interest includes the optimization and control of vehicle automatic transmission systems.

LIN REN is currently pursuing the master's degree with the Chongqing University of Technology, Chongqing, China. His main research interests include the optimization and control of plug-in hybrid electric vehicles and the energy-saving control of vehicle automatic transmission systems.

LIJI XU is currently pursuing the master's degree with the Chongqing University of Technology, Chongqing, China. His main research interests include the control of intelligent vehicles and the control of vehicle automatic transmission systems.

FUTAO SHEN is currently pursuing the master's degree with the Chongqing University of Technology, Chongqing, China. His main research interests include the design and simulation of battery management systems and vehicle battery thermal management.

GUOFANG CHEN is currently pursuing the master's degree with the Chongqing University of Technology, Chongqing, China. Her main research interests include the optimization and control of plug-in hybrid electric vehicles and management and control strategies for brake energy recovery.